R-09-15

Theoretical study of irradiation induced hardening and embrittlement in spent nuclear fuel holders, relevant for the Swedish long-term storage

Nils Sandberg
Division of Reactor Physics,
Royal Institute of Technology (KTH)

Pavel Korzhavyi
Applied Materials Physics,
Department of Materials Science and Engineering,
Royal Institute of Technology (KTH)

April 2009

Svensk Kärnbränslehantering AB
Swedish Nuclear Fuel
and Waste Management Co

Box 250, SE-101 24 Stockholm
Phone +46 8 459 84 00

ISSN 1402-3091
SKB Rapport R-09-15

Theoretical study of irradiation induced hardening and embrittlement in spent nuclear fuel holders, relevant for the Swedish long-term storage

Nils Sandberg
Division of Reactor Physics,
Royal Institute of Technology (KTH)

Pavel Korzhavyi
Applied Materials Physics,
Department of Materials Science and Engineering,
Royal Institute of Technology (KTH)

April 2009

Contents

1 Introduction

Precipitation of Cu particles in α-Fe is a well known problem in pressurized water reactor (PWR) vessels. Depending on the Cu content in the material, precipitation may occur as a result of radiation, potentially leading to embrittlement of the material. Such an accelerated ageing process occurs gradually over the life-time of the reactor, i.e. over time period of several decades. Due to its technological importance, Cu precipitation under irradiation or during thermal ageing has been extensively studied experimentally and theoretically since more than forty years, see Ref. /1/ for a recent review of the current situation on the modelling side.

Recently, Brissoneau and Bocquet /2/, suggested that similar ageing processes may be of relevance also in materials to be used for long-term storage of nuclear waste (see also Ref. /3/). Here, the dose-rate due to activity is much lower compared to that in a reactor. However, because the temperature of interest is also lower (about 100°C compared to 300°C in a PWR), the effect of Cu supersaturation will be stronger, and also the balance between defect production and defect annihilation in the material will be different. The prediction in Refs. /2, 3/ is that, due to gamma-radiation from spent nuclear fuel, a high concentration of small copper particles will form in the steel or cast-iron fuel holders. This, in turn, will lead to an increase in the yield-strength, and as a consequence of that, an increase in the ductileto-brittle transition temperature (DBTT) of roughly 50 K. This increase would occur over 20 to 100 years, and would potentially lead to room-temperature embrittlement. There are no direct experiments with which the predictions in Refs. /2, 3/ can be compared, so they should be regarded as an indication of a potential problem.

The predictions made by Brissoneau *et al.* may be of importance also for the conditions in the Swedish long-term storage. Thus, the aim of the current work is, first, to verify the calculations which underlie the work in Refs. /2, 3/, and second, to review and discuss the models that are used to connect precipitation of Cu particles to changes in the mechanical properties. Finally, we make a rough analytic estimate of the risk of phosphorus segregation to grain boundaries (GB:s) due to irradiation accelerated diffusion. Phosphorus is known to potentially cause GB embrittlement in ferritic steels. In the current case, the segregation of P to GB:s could be accelerated by irradiation induced supersaturation of vacancies, in the same way as Cu precipitation.

2 Results and discussion

The current modelling follows that of Brissonneau *et al.* /3/. It is based on the solution of a set of ordinary differential equations (ODE:s) describing, first, the vacancy-interstitial formation, migration, annihilation and recombination, and second, the precipitation and growth of Cu particles in the matrix. For clarity, we give the details regarding the implementation, and the specification of simulation parameters, in Appendix A. Brissonneau *et al.* considered gamma and neutron activities for two types of fuels, G1 and G4. The damage flux from the G4 fuel is closer to the one calculated by Guinan /4/ for the Swedish spent fuel, so we have chosen to look at the G4 flux. We have a defect production rate

$$g = a\exp(xt) + b\exp(yt) + f \qquad \text{(Eq. 2-1)}$$

with $a = 2.27\times10^{-15}$ dpa/s, $x = -2.850\times10^{-8}$/s, $b = 1.8\times10^{-16}$ dpa/s, $y = -7.4\times10^{-10}$/s and $f = 2\times10^{-20}$/s.

2.1 Vacancy concentration and diffusivity

The production of vacancy-interstitial pairs according to Eq. 2-1 will result in mutual recombination of defects, agglomeration into vacancy or interstitial clusters, and diffusion towards sinks (dislocations and grain boundaries). For the low defect production rate of interest here, vacancy-interstitial recombination and diffusion towards sinks will be dominating. This is described by two coupled equations, one for the vacancy concentration, c_v, and one for the interstitial concentration, c_I. The materials properties that govern the evolution of c_v and c_I are the vacancy and interstitial diffusivities, and the density of sinks, in this case the dislocation density. Details on the numerical implementation of this model are given in Appendix A.

The calculated vacancy concentration for $T = 100$, 150 and 200°C, assuming a defect production rate given in Eq. 2-1, is shown in Figure 2-1. The results compare well with those in Figure 5 in Ref. /3/. We note that, at $T = 100$°C, the equilibrium vacancy concentration, c_v^{th}, with the present parameters, is roughly 20 vacancies/cm^3. In other words, the vacancy supersaturation under the current irradiation conditions, is predicted to be up to 10^{14}. A calculated vacancy concentration can be translated into a corresponding Cu diffusivity, D_{Cu}, according to

$$D_{Cu} = \frac{c_v}{c_v^{th}} D_{Cu}^{th} \qquad \text{(Eq. 2-2)}$$

where D_{Cu}^{th} is the equilibrium Cu diffusivity. This is the basis for irradiation accelerated diffusion and precipitation.

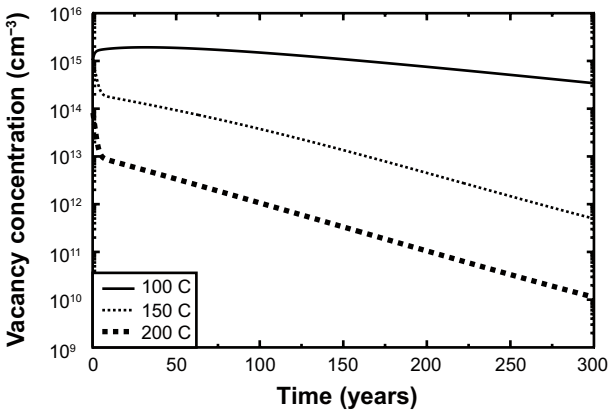

Figure 2-1. *Calculated vacancy concentration for G4 dose rate and at temperatures 100, 150 and 200°C.*

2.2 Precipitation kinetics, thermal ageing

A vacancy supersaturation as seen in Figure 2-1 enables accelerated Cu diffusion according to Eq. 2-2, and potentially Cu particle nucleation and growth, even at 100–200°C. We have simulated this process by methods that are usually applied at higher temperatures, e.g. in pressure vessel applications. Our implementation of the set of ODE:s that describe the evolution of Cu particles (Eq:s A-6) was validated against results by Christien and Barbu /5/. They looked at thermal ageing of a Fe-1.34at%Cu alloy at 500°C, and also compared with experiment. Our calculated mean cluster radius and cluster density are shown in Figure 2-2, and should be compared with Figure 3 in the paper by Christien and Barbu. The parameters used were those in Table A-1 in Appendix A, with exception for the Cu diffusivity, which for the purpose of comparing with the results in Ref. /5/ was set to 7.7×10^{-15} cm^2/s. We find that the agreement between our calculation, and that of Christien and Barbu, is almost perfect.

2.3 Precipitation kinetics during irradiation

The current simulations of Cu cluster precipitation under irradiation was done in the same way as the simulation of thermal ageing, with the exception that the temperature was lower, and the Cu diffusivity was set according to Eq. 2-2. As discussed below, the results are highly sensitive to the numerical values of the Cu diffusion coefficient and the Cu solubility. Those parameters were taken from Ref. /5/, to which Brissonneau *et al.* refer.

The calculated evolution of the mean cluster radius and the cluster density during irradiation at 100°C, and at 150°C, are shown in Figure 2-3 and 2-4, respectively.

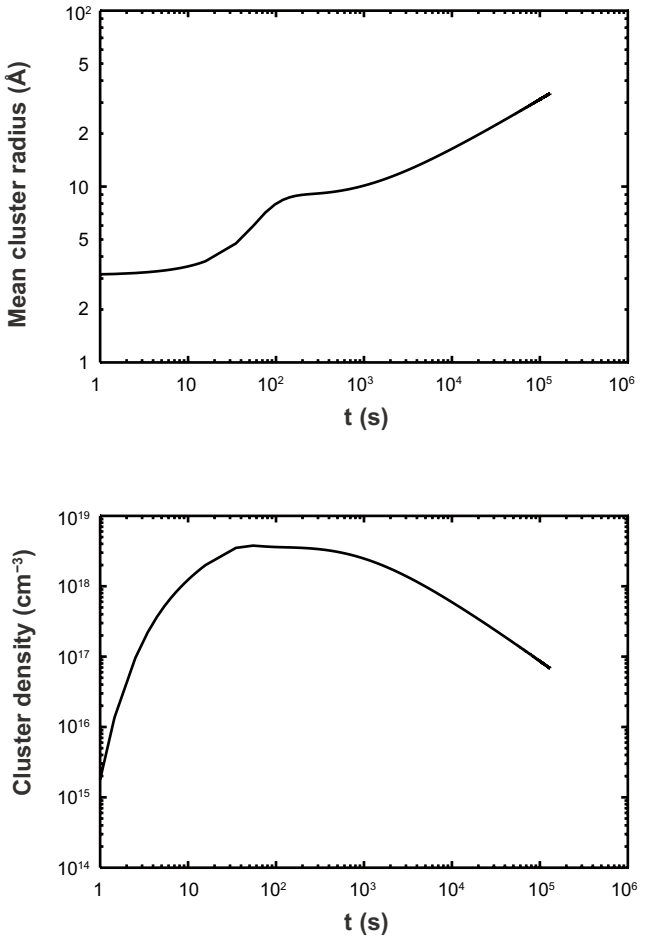

Figure 2-2. *Calculated mean cluster radius and mean cluster density for a Fe1.34at%Cu alloy during thermal aging at 500°C.*

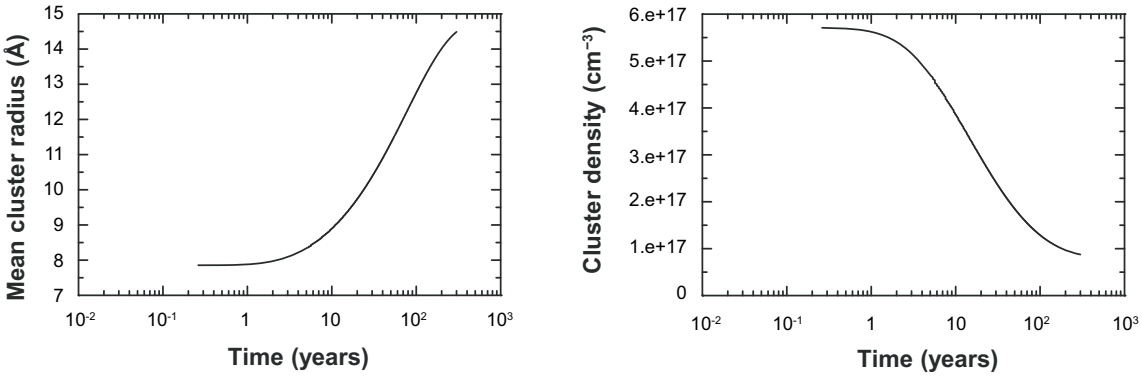

Figure 2-3. *Calculated mean cluster radius and cluster density as a function of time, at T = 100°C.*

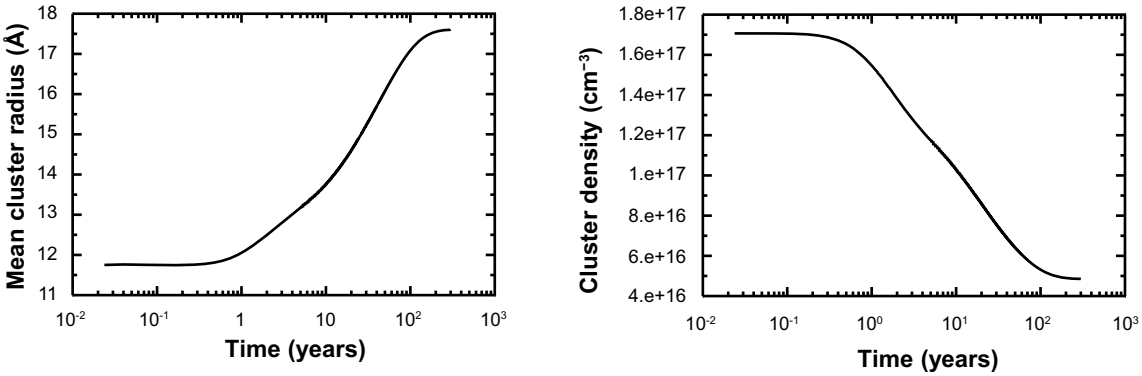

Figure 2-4. *Calculated mean cluster radius and cluster density as a function of time, at T = 150°C.*

By comparing with Figure 6 in Ref. /3/, showing particle concentration versus particle radius for different times, we find that the agreement is reasonably good, although the initial precipitation seems to occur faster in our simulations than shown in Ref. /3/.

2.4 Mechanical effects of precipitation

The precipitation of Cu particles in α-Fe leads to hardening due to dislocation pinning. This was explained by Russel and Brown /6/, who derived the following expression for the increase in shear strength,

$$\Delta\tau = 0.8\frac{Gb}{L}\left[1-\frac{E_1^2}{E_2^2}\right]^{1/2}, \ \sin^{-1}\frac{E_1}{E_2} \leq 50^\circ$$
$$\Delta\tau = \frac{Gb}{L}\left[1-\frac{E_1^2}{E_2^2}\right]^{3/4}, \ \sin^{-1}\frac{E_1}{E_2} \geq 50^\circ \qquad \text{(Eq. 2-3)}$$

Here, G is the Fe shear modulus, b is the Burgers vector, L is the mean planar particle spacing, and $\frac{E_1}{E_2}$ is the energy of the dislocation in the precipitate relative to that in the matrix. Russel and Brown showed that this model is consistent with the maximum increase in yield strength, $\Delta\sigma$, as a function of $f^{1/2}$, where f is the volume fraction of Cu. The same model is used by Brissonneau *et al.* with the difference that, $\frac{1}{L}$ is replaced with $2c_p r_p$, where c_p is the particle concentration and r_p is the radius. This expression differs from that used by Russel and Brown; $\frac{1}{L}=\frac{f^{1/2}}{1.77r_p}$. In the current work, we have accounted for this inconsistency by simply equating the calculated and the experimental yield strength increase for 0.12% Cu at 100°C. In the calculations we have therefore multiplied with a factor 1/1.44 in the calculation of $\Delta\tau$.

Apart from quantifying the maximum yield strength increase, the Russel and Brown model also predicts how the hardening varies as a function of the particle radius. This variation, with parameters for Fe-Cu, is plotted in Figure 2-5. It is seen that the increase in shear strength quickly reaches a maximum at a particle radius $r \approx 10$ Å, and then goes down for $r > 20$ Å.

There are two steps needed to connect the calculated $\Delta\tau$ to a predicted change in ductile-to-brittle transition temperature (DBTT). First, the calculated $\Delta\tau$ is translated into a predicted change in yield stress via the Schmid or Taylor factor f_S

$$\Delta\sigma = f_S \Delta\tau \qquad \text{(Eq. 2-4)}$$

Russel and Brown used a value of $f_S = 2.5$, while Brissoneau *et al.* used $f_S = 3.06$. The uncertainty in f_S is quite large (reasonable values lie between 2.2 and 3.1 for a material with unknown texture /6/). However, the experimental foundation of the Russel and Brown model is the measured increase in yield strength, so an 'error' in the value of f_S does not directly lead to erraneous predictions. The next step made by the authors of Ref. /3/ is to use the correlation between an increase in yield strength and an increase in ductile-to-brittle transition temperature, to conclude that Cu precipitation should embrittle the Fe-Cu alloy. Although this conclusion is based on a well-established empirical correlation, and is consistent with the experimental facts of irradiation-induced embrittlement of pressure-vessel steels, it is not strictly logical. In fact, Russell and Brown themselves, in their original paper /6/, come to the opposite conclusion, namely, that *'alloy systems with attractive particles can give strength without loss in ductility'*. This latter conclusion is only speculative, as its authors admit.

In summary, the model of Russell and Brown gives a fairly accurate description of the effect of copper precipitates on the yield strength of iron-based alloys. It has been shown to slightly overestimate the strengthening effect, in comparison with more sophisticated models such as that of Ref. /7/. The Russell-Brown model is correctly used in Ref. /3/ and gives reasonable numbers, assuming that the simulated precipitate-size distributions are correct. The prediction about an increase in ductile-to-brittle transition temperature may be accepted as qualitatively consistent with experimental facts, but its numerical accuracy is questionable. In the absense of proper theory, the empirical correlation mentioned above is the only means available for making a connection between strength and ductility. The physical nature of this connection is yet to be uncovered.

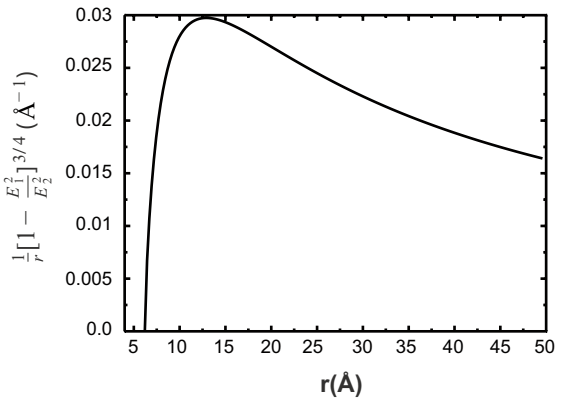

Figure 2-5. *The particle-size dependent factor in Eq. 2-3, for a given volume fraction of precipitate.*

2.5 Predicted shear strength increase

The predicted increase in shear strength according to our calculations, are shown in Figure 2-6 and 2-7, respectively. Our calculations show a faster increase in shear strength $\Delta\tau$ compared to that in Ref. /3/ by a factor of roughly 20, in the case of 0.12% Cu at 150°C. Our predicted evolution in cluster distribution at 150°C is similar to that in Ref. /3/, however, in our modelling the precipitation occurs faster, at least initially. Since the increase in shear strength depends non-linearly on the particle distributions, this results in a much faster initial increase in $\Delta\tau$. However, the conclusion that can still be drawn from Figures 2-3 and 2-4 in combination with Figure 2-5, is that within a period of about 300 years, a very dense Cu cluster distribution is formed, with a mean cluster radius close to the one leading to maximum increase in shear strength. From Figure 2-5 it is seen that the increase is very steep as the particle radius increases, but at the same time, the density of particles decreases. The question whether or not this will happen under the irradiation conditions considered here, will most of all depend on the copper solubility, and the copper diffusion coefficient, as discussed below.

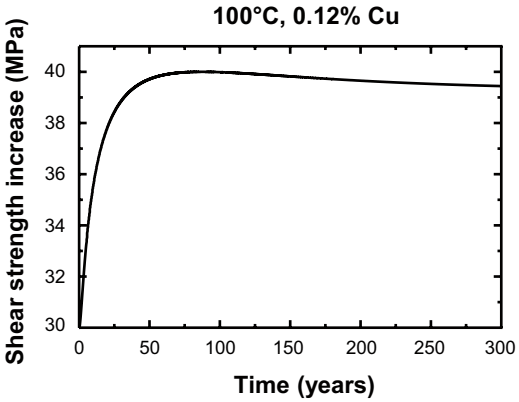

Figure 2-6. *Shear strength increase versus time, at T = 100°C, for 0.12% Cu.*

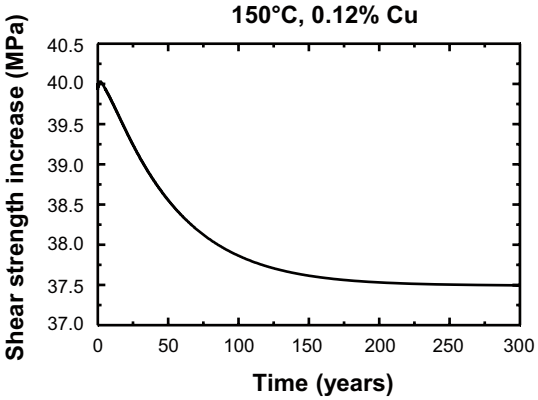

Figure 2-7. *Shear strength increase versus time, at T = 150°C, for 0.12% Cu.*

2.6 Cu diffusivity

In Ref. /5/, the diffusivity is obtained in an indirect way from measurements of Cu precipitation under thermal ageing.

The authors report

$$D_{Cu}(T) = 0.63 \exp(-2.29 \text{ eV}/kT) \text{ cm}^2/\text{s} \quad \text{(Eq. 2-5)}$$

as the best fit. They compare with data given in Salje and Feller-Kneipmeier /8/, more specifically the experiment by Rothmann;

$$D_{Cu}(T) = 5.9 \exp(-2.58 \text{ eV}/kT) \text{ cm}^2/\text{s} \quad \text{(Eq.2-6)}$$

The diffusion parameters (prefactor D_0 and activation energy Q) determining self-diffusion and Cu impurity diffusion in bcc Fe have a variation that depends on the magnetic state of the material, and on the purity of the material, for instance on the C content. Salje and Feller-Kneipmeier report $D_{Cu}(T) = 300 \exp(-2.94 \text{ eV}/kT)$ cm^2/s for high purity (1 ppm C) paramagnetic (PM) Fe-Cu. In the experiment by Rothmann the material contained 40 wppm C. The available diffusion data is mainly for the PM state or for γ (fcc) Fe. It is seen in the experiment by Salje and Feller-Kneipmeier that the diffusivity has a somewhat increased activation energy just below T_C, (1,048 K) just as for Fe self-diffusion. The result is that the diffusivity is decreased below T_C compared with an extrapolation from the PM region.

We note that $D_{Cu}(T)$ is approximately 3–5 times that of Fe self-diffusion over a wide temperature range from the FM to the PM state and over the γ (fcc) region (see the Landolt-Börnstein tables /9, 10/). An extrapolation of the PM data for Cu diffusivity down to near room temperature, leads to a D_{Cu} which is 5–7 orders of magnitude larger than the expected Fe self-diffusion rate.

Experiments with Fe in equilibrium with cementite or graphite should correspond to the high C experiments and, therefore a somewhat lower Q compared with the measurements in high purity Fe as reported by Salje and Feller-Kneipmeier. When extrapolating from temperatures where well controlled experiments are typically done, down to near room temperature, even small changes in Q will have drastic effects. In the work by Christien and Barbu /5/ the activation energy of Cu is lower by 0.6 eV compared to Fe self-diffusion, which translates into an 8 orders of magnitude faster diffusion at 100°C (assuming that the prefactor is the same). While this may certainly be possible, the explanation in terms of atomic mechanisms is still lacking. The kinetics of precipitation (Figures 2-3 and 2-4) as well as the kinetics of the variation in shear strength (Figures 2-6 and 2-7) are proportional to the predicted Cu diffusion coefficient. Considering the large uncertainties in the predicted D_{Cu} under irradiation, it is the single most important parameter in the current modelling.

It should also be mentioned that the mechanisms of Cu diffusion may be qualitatively different in a vacancy supersaturated material, and at low temperatures, as recently shown by Soisson and Fu /11/. In such cases, extrapolations from high-temperature data will not be valid.

2.7 Modelling of phosphorus segregation

Phosphorus is known to potentially cause grain boundary (GB) embrittlement in ferritic steels. In the current case, the segregation of P to grain boundaries could be accelerated by irradiation induced supersaturation of vacancies, in the same way as Cu precipitation. In the following, we use a few simple assumptions in order to estimate this effect.

A P concentration $c_P = 0.01\times10^{-2}$ is assumed. The P "layer" at the GB is taken to be one atom thick, and the GB is assumed to be a perfect sink. Therefore, it is required that atoms a distance $l_{diff,P} = l_{at}/c_P$ away from the GB diffuse to the GB, in order for a substantial build-up of P at the GB to occur. Here, $l_{at} = (1/2)^{(1/3)} a_0 = 2.3\times10^{-10}$ m, which means that $l_{diff,P} = 2.3\times10^{-6}$ m. For one-dimensional diffusion, we have $l \approx \sqrt{(tD)}$, where tD can be replaced witht $\int tD_P(t)dt$. It only remains, therefore, to estimate if the irradiation accelerated diffusion at, $T = 100$°C, is capable of transporting P atoms roughly 2.3×10^{-6} m, or in other words, if $l \gtrsim l_{diff,P} = 2.3\times10^{-6}$ m.

From the Landolt-Börnstein tables /10/, we have, at $T = 100°C$, $D_P = 1\times10^{-42}$, $D_P = 5\times10^{-46}$ or $D_P = 4\times10^{-37}$ m^2/s depending on which experimental data one chooses. The last coefficient refers to paramagnetic Fe, while the first two are for ferro-magnetic Fe. One gets, for $t = 300$ years, $l = 7\times10^{-10}$, $l = 1.5\times10^{-11}$ or $l = 4\times10^{-7}$, depending on which diffusion coefficient that is used. We have assumed a constant vacancy supersaturation of 5×10^{13} and a total time of 300 years.

The conclusion from the above estimate is, that irradiation accelerated P depletion at GB:s is unlikely to take place, assuming a P concentration of 0.01%, unless the P diffusivity at 100°C is of the order of 10^{-37} m^2/s or larger. As with Cu, it is very difficult to estimate D_P at such a low temperature. A hint that the P diffusivity may be unexpectedly large comes from first-principles calculations by Domain and Becquart /12/, who report $D_{Fe} = 2.95\times10^{-7}\exp(-2.66\ \text{eV}/kT)$ m^2/s and $D_P = 4.48\times10^{-7}\exp(-2.30\ \text{eV}/kT)$ m^2/s. These are too large diffusion coefficients when one compares with experiments – a well known deficiency of this type of calculations. However, the *relative* diffusivity may be regarded as more accurate, and assuming $D_{Fe} = 121\times10^{-4}\exp(-2.92\ \text{eV}/kT)$ m^2/s, one finds at $T = 100°C$, $D_P \approx 5\times10^{-37}$ m^2/s, leading to $l \approx 5\times10^{-7}$. Thus, a first estimate using reasonable but highly uncertain assumptions about the P diffusion coefficient at 100°C, leads to the conclusion that P segregation to GB:s is a potential problem in the spent nuclear fuel holders.

3 Conclusions

- The vacancy supersaturations predicted at 100, 150, and 200°C, agree exactly with those calculated in Ref. /3/. A very high vacancy supersaturation (up to 14 orders of magnitude) is predicted, which enables kinetic processes to occur, that would otherwise have been completely frozen in.
- The calculated precipitation kinetics during thermal ageing agrees exactly with previously published results /5/, for the same set of parameters.
- The modelling of strengthening effects due to Cu precipitation that is adopted in Ref. /3/ is equivalent to the model of Russel and Brown, /6/. However, there seem to be an inconsistency in the definition of the mean planar particle spacing, between Russel and Brown, and Brissonneau *et al.* Taking that into account, it is still possible to obtain results and predictions that are consistent with experimental facts.
- Our predicted precipitation kinetics during irradiation at 100 and 150°C, is in general agreement with that found in Ref. /3/. However, the kinetics of the increase in shear strength is overestimated in our work compared to that of Brissonneau *et al.* Nevertheless, the main conclusions below are not changed.
- The simulations show that the supersaturation of Cu is completely precipitated out from the matrix. A high density of small particles form, in the range between 10–20 Å in radius. This is the interval in which the strengthening effect is largest, according to the model of Russel and Brown.
- The two most important factors in the current modelling are the Cu solubility and the Cu mobility at low temperatures (near room temperature). Their extrapolation from experimentally accessible temperature regions is uncertain due to magnetic and other effects. In particular, the effect of the magnetic transition at the Curie temperature can, and should, be included in the analysis.
- The correlation between an increase in yield strength and an increase in ductile-to-brittle transition temperature, used by Brissonneau *et al.* although based on a well established empirical correlation, is not strictly logical. Therefore, the numerical accuracy of this correlation is questionable, and its physical nature is unknown.
- A simple one-dimensional model of P segregation to grain boundaries was derived. It is assumed that P diffusion is accelerated by irradiation in the same way as Cu diffusion is. Using reasonable but highly uncertain assumptions about the P diffusion constant at 100°C, it is concluded that P segregation to grain boundaries may occur.

References

/1/ **Vincent E et al. 2008.** Precipitation of the FeCu system: A critical review of atomic kinetic Monte Carlo simulations, J. of Nuclear materials 373, 387.

/2/ **Brissonneau L, Bocquet J-L, 2003.** Radiation effects on the mechanical properties and long term aging of spent fuel storage containers, Proc. of the 9th international conference on radioactive waste management and environmental remedation 1.

/3/ **Brissonneau L, Barbu A, Bocquet J-L, 2004.** Radiation effects on the long-term ageing of spent fuel storage containers, RAMTRANS 15, 121.

/4/ **Guinan M W, 2001.** Radiation effects in spent nuclear fuel canisters, SKB TR-01-32, Svensk Kärnbränslehantering AB.

/5/ **Christien F, Barbu A, 2004.** Modelling of copper precipitation in iron during thermal aging and irradiation, J. of Nuclear Materials 324, 90.

/6/ **Russel K, Brown L M, 1972.** A dispersion strengthening model based on differing elastic moduli applied to the iron-copper system, Acta Metall, 969.

/7/ **Bacon D J, Osetsky Y N, 2004.** Hardening due to copper precipitates in α-iron studied by atomic-scale modeling, J. Nucl. Mater. 329–333, 1233.

/8/ **Salje G, Feller-Kneipmeier M, 1977.** The diffusion and solubility of copper in iron, J. of Applied Physics 48, 1833.

/9/ **Mehrer H, Stolica N, Stolwijk N A, 1990.** In Self-diffusion in solid metallic elements, Vol. III/26 of Landolt-Börnstein New Series, edited by H. Mehrer (Springer-Verlag, Berlin).

/10/ **Leclaire A D, Neumann G, 1990.** G. In Diffusion of impurities in solid metallic elements, Vol. III/26 of Landolt-Börnstein New Series, edited by H. Mehrer (Springer-Verlag, Berlin).

/11/ **Soisson F, Fu C-C, 2007.** Cu-precipitation kinetics in alpha-Fe from atomistic simulations: Vacancy-trapping effects and Cu-cluster mobility, Phys. Rev. B 76, 214102.

/12/ **Domain C, Becquart C S, 2005.** Diffusion of phosphorus in alpha-Fe: An ab initio study, Phys. Rev. B 71, 214109.

/13/ **Mathon M H et al. 1997.** Experimental study and modelling of copper precipitation under electron irradiation in dilute FeCu binary alloys, J. of Nucl. Mater. 245, 224.

/14/ **Ghoniem N M,Sharafat S, 1980.** A numerical solution to the Fokker-Planck equation describing the evolution of the interstitial loop microstructure during irradiation, J. of Nucl. Mater. 92, 121.

Appendix A

Methods

A.1 Vacancy concentration

Assuming a defect production rate g, the evolution of vacancies and interstitials is given by

$$\frac{dc_v}{dt} = g - k_{rec}\, c_v c_I - D_v z_v \rho_{disl}\, c_v \qquad \text{(Eq. A-1)}$$

$$\frac{dc_I}{dt} = g - k_{rec}\, c_v c_I - D_I z_I \rho_{disl}\, c_I \qquad \text{(Eq. A-2)}$$

where c_v and c_I are the vacancy and interstitial concentrations, k_{rec} is the recombination coefficient, D_v and D_I are the vacancy and interstitial diffusivities, and ρ_{disl} is the dislocation density.

The parameters in Eqs. A-1, A-2 were taken from Ref. /5/. The interstitial migration is much faster than the vacancy migration, and interstitials also annihilate faster than g changes. Therefore, Eq. A-2 can be solved implicitly, which considerably speeds up the simulations.

A.2 Cluster dynamics model

The nucleation and evolution of Cu precipitates is studied using a cluster dynamics model described in Ref. /13/. It models the growth or shrinkage of clusters (in this case, Cu clusters) of size n. The physical parameters that govern their evolution are the diffusivity of Cu, D_{Cu}, and the Fe-Cu mixing energy, $\Omega - TS^{nc}$.

The growth rate of a cluster of size n is given by

$$\beta(n) = 4\pi \left(\frac{3v_a}{4\pi}\right)^{1/3} (n)^{1/3} D_{Cu}\, c_{Cu} / v_a \qquad \text{(Eq. A-3)}$$

The rate of shrinkage of a cluster of size n is

$$\alpha(n) = 4\pi \left(\frac{3v_a}{4\pi}\right)^{1/3} (n-1)^{1/3} D_{Cu}\, c_{Cu,eq} / v_a$$

$$\times \exp\left(\frac{A\sigma}{kT}\left[n^{2/3} - (n-1)^{2/3}\right]\right) \qquad \text{(Eq. A-4)}$$

Here, $A = (36\pi)^{1/3} v_a^{2/3}$ and σ is the surface energy of a precipitate, assumed to be spherical. It is given by

$$\sigma = 1.08 \frac{k_B}{a^2} T_c' \left(1 - \frac{T}{T_c'}\right) \text{ with } T_c' = \frac{1}{2k_B}(\Omega - TS^{nc}) \qquad \text{(Eq. A-5)}$$

The Cu concentrations c_{Cu} and $c_{Cu,eq}$ are the actual and equilibrium concentrations, *per lattice site*. Therefore, we also divide by the atomic volume in Equations A-3 and A-4. This is not done in Ref. /13/ in the expression for the emission rate $\alpha(n)$.

In therms of the combined growth and shrinkage rates, the ODE:s describing the evolution of the Cu cluster distribution read

$$\begin{aligned} \frac{dc_n}{dt} &= \beta(n-1)c_{n-1} + \alpha(n+1)\, c_{n+1} \\ &\quad - [\beta(n) + \alpha(n)]c_n \text{ for } n \le 2, \\ \frac{dc_1}{dt} &= \sum_{n=2}^{\infty} \alpha(n)c_n - \sum_{n=2}^{\infty} \beta(n)c_n \\ &\quad - 2\beta(1)c_1 + \alpha(2)c_2 \text{ for } n = 1 \end{aligned} \qquad \text{(Eq. A-6)}$$

Equations A-6 were rewritten in a continuous form (Fokker-Planck equations) and solved on a grid with increasing step-length for large n, as described in Ref. /14/.

A.3 Parameters of the current simulations

The parameters that were used in the current work were taken from Ref. /5/. They are listed in Table A-1.

Table A-1. Parameters used in the current simulations.

Ω/k	6,255 K
S^{nc}/k	0.866
D_{Cu}	$0.63\exp(-2.29\text{eV}/kT)$ cm^2/s
$D_{Fe,self}$	$1\exp(-2.9\text{eV}/kT)$ cm^2/s
E_v^f	1.6 eV
E_v^m	1.3 eV
E_I^f	4.3 eV
E_I^m	0.3 eV
$D_{v,0}$	1 cm^2/s
$D_{I,0}$	4×10^{-4} cm^2/s
k_{rec}	corresponds to r_{rec} 6.5 Å
ρ_{disl}	10^8/cm^2